processes

MDPI

Article

Electrocoagulation Coupled with TiO_2 Photocatalysis: An Advanced Strategy for Treating Leachates from the Degradation of Green Waste and Domestic WWTP Biosolids in Biocells

Rodny Peñafiel [1,*], Nelly Esther Flores Tapia [1,*], Celia Margarita Mayacela Rojas [2], Freddy Roberto Lema Chicaiza [3] and Lander Pérez [1]

[1] Environmental Laboratory, Faculty of Food Science and Biotechnology Engineering, Universidad Técnica de Ambato, Ambato 180206, Ecuador; lv.perez@uta.edu.ec
[2] Faculty of Engineering, National University of Chimborazo, Riobamba 060108, Ecuador; celia.mayacela@unach.edu.ec
[3] Industrial Engineering Program, Faculty of Systems, Electronics and Industrial Engineering, Universidad Técnica de Ambato, Ambato 180206, Ecuador; fr.lema@uta.edu.ec
* Correspondence: rd.penafiel@uta.edu.ec (R.P.); nellyflorestapia@gmail.com (N.E.F.T.)

Abstract: Leachates generated from the degradation of green waste and biosolids from urban wastewater treatment plants (WWTPs) pose significant environmental concerns due to high concentrations of organic pollutants and heavy metals. This study proposes a hybrid treatment strategy combining electrocoagulation (EC) and UVC-activated TiO_2 photocatalysis to remediate leachates produced in laboratory-scale biocells. Initial characterization revealed critical pollutant levels: COD (1373 mg/L), BOD_5 (378 mg/L), total phosphorus (90 mg/L), ammoniacal nitrogen (201 mg/L), and metals such as Ni, Pb, and Mn levels all exceeding those set out in the Ecuadorian discharge regulations. Optimized EC achieved removal efficiencies of 62.6% for COD, 44.4% for BOD_5, 89.8% for phosphorus, and 86.2% for color. However, residual contamination necessitated a subsequent photocatalytic step. Suspended TiO_2 under UVC irradiation removed up to 81.8% of the remaining COD, 88.7% of the ammoniacal nitrogen, and 94.4% of the phosphorus. Levels of heavy metals such as Zn, Fe, Pb, Mn, and Cu were reduced by over 80%, while Cr^{6+} was nearly eliminated. SEM–EDS analysis confirmed successful TiO_2 immobilization on sand substrates, revealing a rough, porous morphology conducive to catalyst adhesion; however, heterogeneous titanium distribution suggests the need for improved coating uniformity. These findings confirm the potential of the EC–TiO_2/UVC hybrid system as an effective and scalable approach for treating complex biocell leachates with reduced chemical consumption.

Keywords: electrocoagulation; photocatalysis; TiO_2; leachate treatment; biocells; UVC radiation; advanced oxidation processes; heavy metals; nitrogen removal; SEM–EDS analysis

check for updates

Academic Editors: Bruno Ramos, Mohamed Gar Alalm and Antonio Carlos Silva Costa Teixeira

Received: 16 April 2025
Revised: 16 May 2025
Accepted: 23 May 2025
Published: 2 June 2025

Citation: Peñafiel, R.; Flores Tapia, N.E.; Mayacela Rojas, C.M.; Lema Chicaiza, F.R.; Pérez, L. Electrocoagulation Coupled with TiO_2 Photocatalysis: An Advanced Strategy for Treating Leachates from the Degradation of Green Waste and Domestic WWTP Biosolids in Biocells. *Processes* **2025**, *13*, 1746. https://doi.org/10.3390/pr13061746

Copyright: © 2025 by the authors. Licensee MDPI, Basel, Switzerland. This article is an open access article distributed under the terms and conditions of the Creative Commons Attribution (CC BY) license (https://creativecommons.org/licenses/by/4.0/).

1. Introduction

Water contamination is a critical global environmental and public health concern and is driven by increasing anthropogenic activities and the generation of hazardous waste. One of the most significant sources of such contamination is landfill leachate—an effluent with high chemical complexity and toxicity, produced by the decomposition of organic waste. These leachates frequently contain elevated concentrations of heavy metals, persistent organic pollutants (POPs), and emerging contaminants, posing serious risks to ecosystems and human health [1]. In cities such as Ambato, Ecuador, the management of green waste and

biosolids generated by urban wastewater treatment plants (WWTPs) remains a significant environmental challenge. The biological degradation of these materials generates leachates that can infiltrate ground and surface water if not properly treated [2,3].

Biocells have emerged as an in situ landfill management strategy that accelerates organic matter degradation through leachate recirculation and air injection, enhancing microbial activity [4,5]. However, landfill leachates typically present complex chemical compositions, characterized by high concentrations of COD, ammoniacal nitrogen, and heavy metals, as well as recalcitrant organic compounds such as phenols, pharmaceuticals, and persistent organic pollutants (POPs) [6,7]. Conventional WWTPs were not originally designed to eliminate such persistent or complex contaminants and, as a result, often demonstrate limited removal efficiency. Moreover, the high loads of recalcitrant pollutants in biocell leachates may interfere with biological treatment processes, ultimately compromising overall treatment performance [8].

Advanced oxidation processes (AOPs), such as photocatalysis (PC), particularly when combined with electrocoagulation (EC), have emerged as effective technologies for treating complex effluents such as biocell leachates. EC promotes pollutant removal through the in situ generation of coagulants via anodic dissolution [9,10]. Photocatalysis with TiO_2 activated by UVC radiation enables mineralization of recalcitrant organic matter through hydroxyl radical generation, with UVC providing enhanced quantum efficiency compared to longer wavelengths [11–13]. TiO_2 can be applied either in suspension for high activity or immobilized to simplify catalyst recovery, though immobilization often reduces efficiency [14].

Recent studies have explored hybrid photocatalysts and modified TiO_2 systems to enhance the degradation of POPs, including pesticides and pharmaceuticals. For instance, Yarbay et al. [15] reported the efficient degradation of the neonicotinoid insecticide imidacloprid using a mesoporous silica material (SBA-15) doped with cadmium, iron, and titanium dioxide. The optimal photocatalytic performance was achieved with the uncalcined 10% Cd/SBA-15 formulation. Similarly, Anucha et al. [16] developed a molybdenum-doped TiO_2 photocatalyst for the degradation of carbamazepine (CBZ), a pharmaceutical contaminant of emerging concern, achieving over 99% removal under UV irradiation.

Despite growing interest in hybrid systems, few studies have explored their application to leachates generated from biocells treating green waste and WWTP biosolids. This research gap underscores the need for optimized treatment approaches tailored to the specific characteristics of these effluents. In this context, combining EC and PC holds the potential to overcome the limitations of each individual process. EC pre-treatment improves optical clarity and reduces metal load, thereby enhancing the effectiveness of subsequent photocatalytic oxidation [17].

This study investigates the performance of a hybrid electrocoagulation–photocatalysis (EC–PC) treatment system applied to biocell leachates generated under controlled laboratory conditions using green waste and WWTP biosolids. Both suspended and sand-immobilized TiO_2 photocatalyst configurations were assessed, with key operational parameters—including pH, TiO_2 concentration, leachate dilution, and H_2O_2 dosage—systematically optimized. To support the characterization of the immobilized photocatalyst, scanning electron microscopy (SEM) and energy-dispersive X-ray spectroscopy (EDS) analyses were conducted. These techniques provided detailed insight into surface morphology, porosity, and titanium distribution. The proposed hybrid approach demonstrated enhanced treatment efficiency and may represent a cost-effective and scalable alternative in scenarios where advanced technologies such as ozonation or membrane filtration are economically or operationally unfeasible. This work contributes to

the development of accessible, context-adapted treatment solutions for sustainable leachate management in low-resource regions.

2. Materials and Methods

2.1. Analytical Methods for Biocell Leachate Characterization

Standard methods were applied to evaluate leachate quality before and after the treatment processes. General water quality parameters, including pH, electrical conductivity, and turbidity, were measured using a multiparameter probe (HI 9829, Hanna Instruments Inc., Woonsocket, RI, USA), following APHA Standard Methods (SM 4500 B, SM 2510 B, and SM 2130 B) [18]. Chemical oxygen demand (COD) and Total nitrogen were determined using a multiparameter photometer (HI 83399, Hanna Instruments Inc., Woonsocket, RI, USA), applying methods SM 5220 D and SM 4500-N. Ammonium, nitrate, total phosphorus, fluoride, chloride, sulfate, and heavy metals (Cr, Zn, Fe, Pb, Cd, Ni, As, Mn, and Cu) were quantified through spectrophotometric and atomic absorption techniques (SM 4500-P, SM 3113 B, and EPA 315 B). Biochemical oxygen demand (BOD_5) was analyzed using an OxiTop IS 6 WTW system (WTW, Xylem Analytics Germany Sales GmbH & Co. KG, Weilheim, Germany), following method SM 5210 D. Total, suspended, and dissolved solids were determined using gravimetric methods (SM 2540 B, C, and D). Post-treatment characterization was conducted to compare pollutant removal efficiency, ensuring compliance with Ecuadorian environmental discharge standards, TULSMA [19].

2.2. Implementation of Biocells for Green Waste and Biosolid Degradation

Three laboratory-scale biocells were implemented using polyvinyl acrylic columns for the degradation of green waste and biosolids from the Ambato Wastewater Treatment Plant (WWTP) (Figure 1). Each column was conditioned with layers of sand, compost, and organic waste, facilitating microbial activity and biogas production [20]. Leachate recirculation was carried out using peristaltic pumps to maintain optimal moisture conditions, enhance organic matter stabilization, and facilitate the removal of biodegradable organic compounds from the leachate [21].

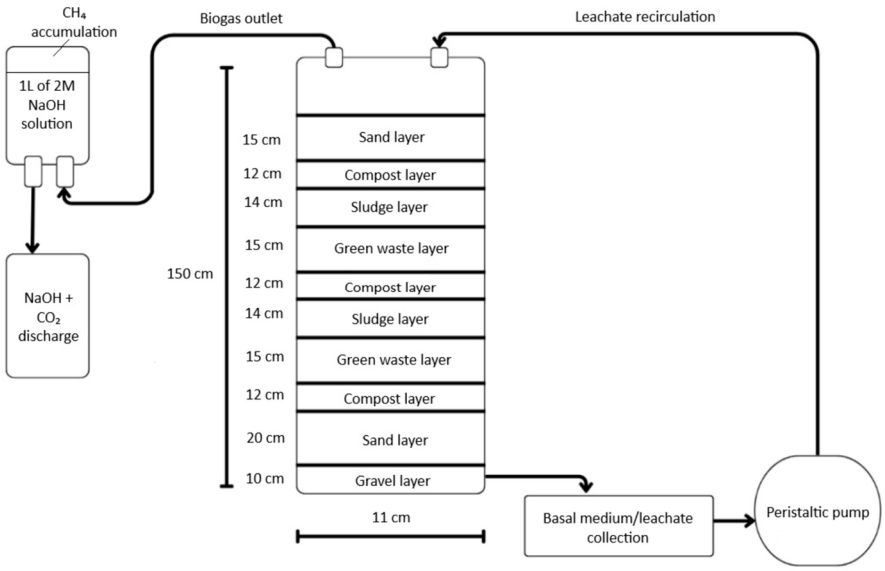


Figure 1. Laboratory-scale biocells for green waste and biosolid degradation.

During a 12-week operation period, the quality of the generated leachate was evaluated in terms of organic matter concentration (COD and BOD_5), ammoniacal nitrogen, and heavy metals (Mn, Cd, Ni, and Pb). Biological treatments are a well-established

technology for effectively removing pollutants from leachate [22]; however, additional treatment steps may be necessary to ensure compliance with Ecuadorian effluent discharge regulations. Therefore, after 12 weeks, the biocell leachate was subsequently treated using electrocoagulation coupled with UVC–TiO_2 photocatalysis.

2.3. Biocell Leachate Pre-Treatment Using Electrocoagulation

Electrocoagulation was conducted as a pre-treatment process for biocell leachate to reduce organic matter, suspended solids, and ammonium nitrogen prior to the photocatalytic treatment. A series of batch experiments were performed using 100 mL of leachate, applying different current densities. Electrocoagulation was conducted in a 20 cm^2 electrochemical reactor equipped with AISI 314 stainless steel electrodes (Metalmet, Quito, Ecuador), separated by 1 cm, and operated without agitation. The applied current intensities ranged from 100 to 2000 mA, and COD measurements were taken at 15, 30, 45, and 60 min by collecting 6 mL samples at each interval for analysis. Electrocoagulation pre-treatment effectively removes organic matter, suspended solids, and a portion of ammonium nitrogen. To further reduce ammonium nitrogen levels, air stripping is performed under alkaline conditions (pH = 12), facilitating its removal and lowering its concentration to below 10 mg/L.

2.4. Optimization of Photocatalytic Treatment for Electrocoagulation Pre-Treated Leachate

The photocatalytic treatment was applied to leachate pre-treated by electrocoagulation and subsequently filtered using a 1.0 µm glass fiber filter (GF1, CHMLAB Group, Barcelona, Spain). The process utilized a UVC radiation source (Toshiba Corporation, Tokyo, Japan) with wavelengths of 180 nm and 254 nm, along with suspended TiO_2 (Degussa P25, Evonik Industries, Essen, Germany) in a batch reactor (Figure 2).

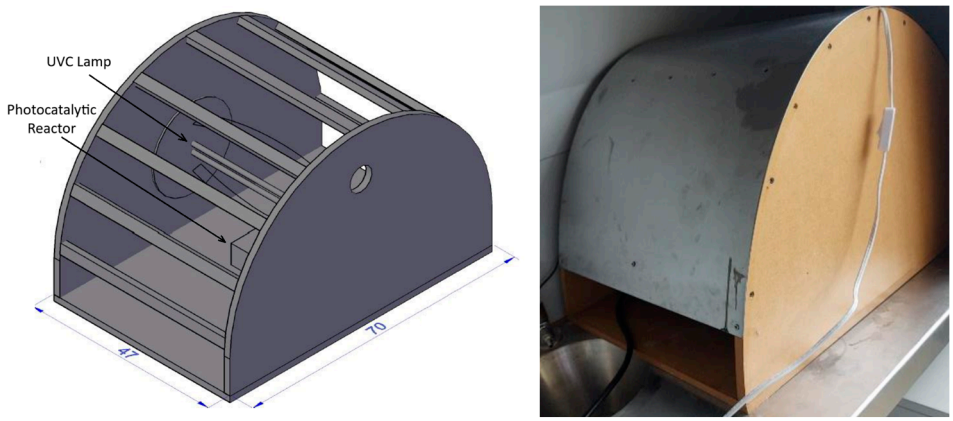


Figure 2. UVC–TiO_2 batch photocatalytic reactor using TiO_2 in suspension; dimensions in cm.

Color removal was selected as the optimization parameter due to its rapid and straightforward determination. A five-stage experimental design was implemented to investigate key process variables influencing treatment efficiency, including initial pH, hydrogen peroxide (H_2O_2) concentration, TiO_2 concentration, leachate dilution, and UVC radiation intensity. In the first stage, the effect of initial pH on removal efficiency was assessed at 5.6, 8, and 10, with a 1:4 leachate dilution, 8 g/L of TiO_2, no addition of H_2O_2, and a 20-min exposure to a 30 W UVC lamp positioned 9.5 cm from the photoreactor (UVC radiation intensity of 1554.2 W/cm^2). In the second stage, the influence of H_2O_2 concentration (2, 20, 100, 200, and 400 mg/L) was analyzed under the optimal pH condition established in the previous phase. The third stage examined the effect of TiO_2 concentration in suspension (2, 4, 8, and 12 g/L), while the fourth stage evaluated the impact of leachate dilution (1:4,

1:3, 1:2, and 1:1). Finally, in the fifth stage, two UVC radiation intensities were compared: 1554.2 W/cm^2 (lamp at 9.5 cm) and 2801 W/cm^2 (lamp at 4.5 cm). UVC intensities were measured using a UV light meter (Model SDL470, Extech Instruments, Nashua, NH, USA). The experimental results were analyzed using Analysis of Variance (ANOVA) to determine the statistical significance of each variable in color removal.

2.5. Photocatalytic Treatment Using Sand-Immobilized TiO_2

Titanium dioxide (TiO_2) was immobilized on natural aluminosilicate sand (A3 grade, supplied by RELUBQUIM, Quito, Ecuador) with a particle size range of 6–12 mm. According to the supplier, this material is primarily composed of silica (SiO_2) and alumina (Al_2O_3), and is widely used in filtration and wastewater treatment systems due to its chemical inertness and mechanical resistance. The thermal fixation procedure consisted of drying at 105 °C for 24 h, impregnation with a TiO_2 suspension (1 g/L), and annealing at 500 °C for 2 h, in accordance with methods reported in previous studies that indicate this temperature ensures optimal adhesion and photocatalytic performance of TiO_2 coatings on granular supports without compromising the support integrity [23,24].

Photocatalytic experiments using TiO_2 immobilized on sand were conducted in both batch and continuous-flow reactors. The batch reactor consisted of a glass Petri dish (11 cm in diameter and 1 cm in height) with a fixed layer of TiO_2-coated sand at the bottom. An amount of 20 mL of leachate was added to the batch reactor until the sand was fully submerged in the liquid. A plastic mesh was positioned to support a magnetic stirrer, ensuring continuous agitation during UVC irradiation (Figure 3). The lamp was enclosed within a protective housing to prevent direct exposure to UVC radiation.



Figure 3. Continuous-flow reactor using sand-immobilized TiO_2.

The experimental conditions for pH, TiO_2 loading, UVC irradiance, and H_2O_2 concentration, optimized in the previous section, were applied to the photocatalytic treatment. After 2 h of treatment, the removal of color and chemical oxygen demand (COD) was evaluated.

In the continuous-flow reactor experiments, the system was designed with 12 internal channels (2 cm width) to facilitate a zigzag leachate flow through a 2 cm-thick TiO_2-coated sand layer. The reactor contained 4 L of immobilized TiO_2-coated sand and operated at a flow rate of 5 mL/min, controlled by peristaltic pumps, with a residence time of approximately 2 h (Figure 4).

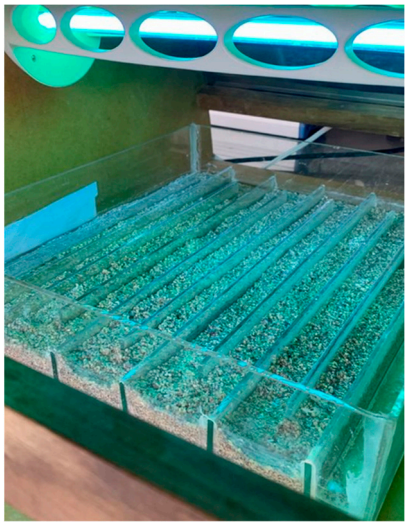


Figure 4. Photocatalytic continuous-flow reactor using TiO_2 immobilized on sand.

The applied UVC irradiance was approximately 700 $\mu W/cm^2$, with an H_2O_2 concentration of 80 mg/L and a leachate dilution ratio of 1:10.

2.6. Scanning Electron Microscopy (SEM) and Elemental Surface Analysis (EDS) of TiO_2-Coated Sand

The surface morphology of the TiO_2-coated sand support was analyzed using scanning electron microscopy (SEM) in combination with energy-dispersive X-ray spectroscopy (EDS). Imaging and elemental analyses were performed using a Phenom ProX desktop SEM system (Model 1255, Thermo Fisher Scientific, Waltham, MA, USA) equipped with an integrated EDS module. Samples were prepared by mounting dry TiO_2-coated sand particles on adhesive carbon tape fixed to aluminum stubs. SEM micrographs were acquired at magnifications ranging from 140× to 6700×, using accelerating voltages of 5 kV and 15 kV, respectively. Low-magnification images (140× and 730×) were used to evaluate macrostructural porosity and the distribution of the TiO_2 coating, while high-magnification images (5800× and 6700×) enabled visualization of fine TiO_2 aggregates and their anchoring to the substrate's microtopography.

Elemental mapping was conducted to assess the spatial distribution of titanium and other relevant elements (O, Si, Al, Na, and K) across selected surface regions. Additionally, elemental mapping by EDS in uncoated regions of the sand grains was used to infer the chemical composition of the support material, confirming an aluminosilicate matrix typical of natural siliceous sands. Point analyses were performed at specific locations to quantify localized Ti accumulation. EDS spectra and elemental maps were processed using Phenom ProSuite Element Identification software (version 2.3, Thermo Fisher Scientific, Waltham, MA, USA), and the results were reported as weight percentages (wt%).

3. Results and Discussion

3.1. Biocell Leachate Characterization

The physicochemical characterization of the raw biocell leachate, presented in Table 1, reveals high pollutant levels that do not comply with Ecuadorian discharge limits. Nevertheless, it exhibits a composition typical of semi-stabilized leachates [25].

Table 1. Physicochemical characterization of raw biocell leachate.

Parameter	Units	Raw Biocell Leachate	Ecuadorian Freshwater Body Regulations	Typical Leachate Composition [22]
pH		8.98 ± 0.01	6–9	4.5–9.0
Color	PCU	7733 ± 289	-	2–25
COD	mg/L	1373 ± 55	200	500–30,000
BOD_5	mg/L	378 ± 44	100	100–5000
Total Solids	mg/L	12,835 ± 43	1600	1000–50,000
Total Suspended Solids	mg/L	208 ± 7	130	200–5000
Total Nitrogen (TN)	mg/L	393 ± 5	-	10–3000
Ammonia (NH_3-N)	mg/L	201 ± 0.6	30	10–2000
Nitrate (NO_3^-)	mg/L	n/d	-	0.1–50
Total Phosphorus (TP)	mg/L	90 ± 1	10	0.1–50

n/d = not detected.

The physicochemical characterization of the raw biocell leachate (Table 1) indicates a composition consistent with semi-stabilized leachates [25]. The leachate exhibits a moderately alkaline pH of 8.98 ± 0.01, typical of mature landfill leachates. Critical pollution indicators—COD and BOD_5—were measured at 1373 ± 55 mg/L and 378 ± 44 mg/L, respectively, with both substantially exceeding Ecuadorian freshwater discharge limits (200 mg/L and 100 mg/L). The low BOD_5/COD ratio (0.28) suggests the presence of poorly biodegradable organic matter, highlighting the need for advanced oxidation or hybrid treatment processes [26]. Nitrogenous compounds were also present at critical levels (total nitrogen reached 393 ± 5 mg/L and ammoniacal nitrogen 201 ± 0.6 mg/L), both of which surpass typical regulatory thresholds (e.g., 60 mg/L for TN). These values raise serious environmental concerns due to the risk of aquatic toxicity and eutrophication [27]. Additionally, the total phosphorus concentration of 90 ± 1 mg/L greatly exceeds the national limit of 10 mg/L, further supporting the need for effective nutrient removal strategies before environmental discharge.

The characterization of heavy metals in the raw biocell leachate, as shown in Table 2, reveals substantial exceedances of Ecuadorian freshwater discharge regulations, underscoring the environmental risks associated with its direct disposal. Concentrations of nickel (7.063 mg/L), lead (0.633 mg/L), and manganese (4.67 mg/L) exceed regulatory thresholds by 253%, 216%, and 134%, respectively. Cadmium (0.043 mg/L) also surpasses the limit of 0.02 mg/L, further emphasizing the need for an effective heavy metal removal strategy. In contrast, chromium VI (0.122 mg/L), arsenic (0.031 mg/L), and zinc (2.6 mg/L) remain within acceptable regulatory limits. Compared to the concentration ranges reported by Teng et al. [21] for typical aged landfill leachates, the biocell leachate exhibits markedly elevated levels of nickel, manganese, and lead, which generally remain below 1 mg/L in conventional landfill environments. This enrichment is likely attributable to the co-disposal of biosolids from the Ambato wastewater treatment plant (WWTP), which may introduce additional trace metals into the leachate matrix. Similarly, values reported by Wang and Qiao [22] indicate that the concentrations of copper (0.97 mg/L) and cadmium (0.043 mg/L) in the biocell leachate exceed the upper bounds commonly observed in municipal landfill leachates, while zinc and chromium remain within expected ranges. Iron, at 1.7 mg/L, falls within the broad interval of 0.019–38.73 mg/L reported in the literature, though continuous monitoring remains advisable.

Table 2. Heavy metal concentrations in raw biocell leachate compared to Ecuadorian discharge standards.

Parameter	Units	Raw Biocell Leachate	Ecuadorian Freshwater Body Regulations	Typical Leachate Composition [22]
Zn	mg/L	2.6 ± 0.2	5	2.56
Fe	mg/L	1.7 ± 0.17	10	0.019–38.73
Cd	mg/L	0.043 ± 0.001	0.02	<1
Ni	mg/L	7.063 ± 0.022	2	<1
Cr^{6+}	mg/L	0.122 ± 0.002	0.5	<1
Cr_{TOTAL}	mg/L	0.956 ± 0.020	-	<1
Pb	mg/L	0.633 ± 0.012	0.2	<1
As	mg/L	0.031 ± 0.001	0.1	<1
Mn	mg/L	4.67 ± 0.58	2	-
Cu	mg/L	0.97 ± 0.12	1	<1

These deviations highlight the complexity of biocell leachates and the potential environmental hazards of untreated discharge. The elevated concentrations of nickel, lead, and manganese—known for their toxicity and bioaccumulative potential—pose a considerable risk to aquatic ecosystems and may lead to long-term ecological degradation if not adequately treated [28]. The metal profile, together with the presence of poorly biodegradable organic matter, supports the adoption of a multi-stage treatment strategy. This should include physicochemical metal removal processes (e.g., electrocoagulation and/or adsorption) coupled with advanced oxidation technologies such as TiO_2 photocatalysis to address recalcitrant organic pollutants. Although some metals, such as chromium VI and arsenic, remain within permissible limits, their environmental persistence warrants ongoing monitoring. Overall, the findings underscore the need for targeted and site-adapted remediation strategies to ensure regulatory compliance and safeguard receiving water bodies.

3.2. Biocell Leachate Decontamination Using Electrocoagulation

The optimization of electrocoagulation for biocell leachate treatment was carried out to achieve maximum COD removal efficiency while maintaining an energy-efficient process. The selected operational parameters were an electrode area of 20 cm^2, a treatment time of 60 min, and an electrode spacing of 1 cm, using AISI 314 stainless steel electrodes (Metalmet, Quito, Ecuador) without stirring. These parameters were maintained constant to isolate the effect of current intensity on COD removal.

The results presented in Figure 5 indicate that increasing current intensity enhances COD removal, peaking at approximately 1000 mA (50 mA/cm^2, $\Delta V_{average}$ = 15.4 V) with a removal efficiency of 53.4%. However, a further rise to 2700 mA (135 mA/cm^2, $\Delta V_{average}$ = 31.5 V) reduces COD removal to 45.6%. This behavior can be attributed to side reactions, excessive gas evolution, and possible electrode passivation, which diminish the effectiveness of electrocoagulation at higher current densities [29].

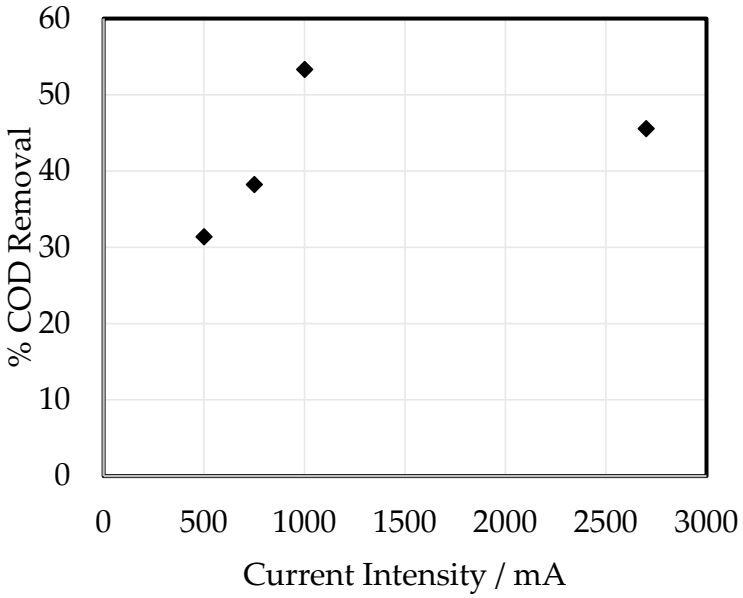


Figure 5. Effect of current intensity on COD removal during electrocoagulation.

To balance COD removal efficiency and energy consumption, a current intensity of 500 mA (25 mA/cm^2, $\Delta V_{average} = 5.7$ V) was selected, resulting in a more favorable energy demand (28.3 kWh/m^3) compared to higher current intensities—69.4 kWh/m^3 at 750 mA, 153.5 kWh/m^3 at 1000 mA, and 850.5 kWh/m^3 at 2700 mA. These results are consistent with those reported by Jallouli et al. [30], who observed an energy consumption of 33.33 kWh/m^3 during the electrocoagulation of tannery wastewater. The selection of 500 mA was based on the highest ratio of COD removal efficiency to energy consumption (8.0% per kWh/m^3), supporting a more energy-efficient and sustainable treatment strategy [31].

Under these conditions, electrocoagulation achieved a 62.6% reduction in COD (from 1373 mg/L to 513 mg/L), a 44.4% reduction in BOD_5 (from 378 mg/L to 210 mg/L), and 89.8% removal of total phosphorus, Table 3. However, ammoniacal nitrogen (N-NH_3) removal was limited to only 17.9%, which remained insufficient to meet freshwater discharge limits. Rookesh et al. [32] reported that the electrocoagulation of leachate using Fe/Gr electrodes under following conditions—a pH of 7.5, a current density of 64 mA/cm^2, an inter-electrode distance of 1.5 cm, an electrolysis time of 120 min—achieved a COD removal efficiency of 30.63%, which is lower than the 62.6% removal efficiency observed in this study. Nevertheless, regarding color and ammonia (N-NH_3) removal, Rookesh et al. [32] achieved efficiencies of 96.51% and 83.67%, respectively, which are higher than the 86.2% and 17.9% efficiencies reported in the present study.

Metals were removed by electrocoagulation, achieving final concentrations that comply with freshwater body regulations, as shown in Table 4. Lead (86.9%), cadmium (71.9%), and copper (82.5%) concentrations were reduced to levels below regulatory limits, while hexavalent chromium, with a removal efficiency of 50.8%, complied with discharge limits despite its moderate reduction. Zailani and Zin [10] reported metal removal efficiencies ranging from 83% to 99%, results that align with the findings of the present study. In addition, Khan et al. [33] reported metal removal efficiencies for various heavy metals using electrocoagulation, achieving 99.9% for iron (Fe), zinc (Zn), manganese (Mn), and copper (Cu), 98% for nickel (Ni), 96% for cadmium (Cd), and 88% for chromium (Cr).

Table 3. Pollutant removal efficiency after electrocoagulation treatment.

Parameter	Unit	Treated Leachate	% Removal	Freshwater Body Regulation
pH		10.3 ± 0.04	-	6–9
Color	PCU	1068 ± 6	86.2	-
COD	mg/L	513 ± 6	62.6	200
BOD_5	mg/L	210 ± 3	44.4	100
Total Solids (TS)	mg/L	11,953 ± 30	6.9	1600
Total Nitrogen (TN)	mg/L	240 ± 1	38.9	-
Ammonia (N-NH_3)	mg/L	165 ± 1	17.9	30
Nitrate (NO_3^-)	mg/L	n/d	-	-
Total Phosphorus (TP)	mg/L	9.2 ± 0.1	89.8	10

n/d = not detected.

Table 4. Heavy metal removal efficiency after electrocoagulation treatment.

Parameter	Unit	Treated Leachate	% Removal	Freshwater Body Regulation
Zn	mg/L	0.04 ± 0.01	98.5	5
Fe	mg/L	1.23 ± 0.02	27.7	10
Cd	mg/L	0.0121 ± 0.001	71.9	0.02
Cr^{6+}	mg/L	0.06 ± 0.001	50.8	0.5
Cr_{TOTAL}	mg/L	0.5707 ± 0.004	40.3	-
Pb	mg/L	0.0828 ± 0.004	86.9	0.2
Mn	mg/L	1.67 ± 0.06	64.2	2
Cu	mg/L	0.17 ± 0.01	82.5	1

3.3. Optimization of Photocatalytic Decontamination for Electrocoagulation Pre-Treated Leachate

The optimization of photocatalytic decontamination was conducted on leachate pre-treated through electrocoagulation, followed by air stripping to reduce ammoniacal nitrogen (N-NH_3) to below 10 mg/L. The study evaluated pH, H_2O_2 concentration, TiO_2 dosage, leachate dilution, and UVC radiation intensity to enhance treatment efficiency. For the optimization study of parameters, the UVC radiation time was kept constant at 20 min. The results of color removal were analyzed using the statistical technique of Analysis of Variance (ANOVA) and are presented in Table 5.

The table indicates that all treatments are significantly different, as their *p*-values from the ANOVA analysis are below 0.05. Regarding treatment efficiency, the highest color removal efficiency was achieved at pH 5.6. In contrast, higher pH values (8 and 10) led to reduced efficiency, dropping to 54.4% and 30.5%, respectively. This result can be attributed to the surface charge of TiO_2, which is positively charged at pH 5.6, thereby enhancing the adsorption of organic compounds that are predominantly negatively ionized under slightly acidic conditions [34]. Moreover, the optimal H_2O_2 concentration (200 mg/L, H_2O_2/COD ratio of 1.6) achieved 88.5% color removal; however, increasing it to 400 mg/L (H_2O_2/COD ratio of 3.2) slightly reduced efficiency to 86.3%, likely due to radical scavenging effects [35]. Regarding the influence of TiO_2 concentration, the highest efficiency (88.5%) was observed at 8 g/L TiO_2. However, higher catalyst concentrations resulted in only a minor increase

in removal efficiency (87.7%), which can be attributed to reduced UVC light penetration due to particle agglomeration and increased suspension opacity, consequently limiting the photocatalytic degradation of organic compounds [36]. Similarly, a 1:4 dilution ratio yielded the best results, achieving 88.5% color removal, whereas increasing the organic load through lower dilution ratios (1:3, 1:2, and 1:1) led to a progressive decline in removal efficiency [37]. Finally, the effect of UVC radiation intensity was evaluated, revealing that a higher intensity (2801 W/cm^2) provided only a slight improvement in color removal (88.7%) compared to 1554 W/cm^2 (88.5%) [38].

Table 5. Effect of process variables on color removal from electrocoagulation pre-treated leachate.

pH	**5.6**	**8**	**10**			**Analysis of Variance, *p*-Value**
%R (color)	83.2	54.4	30.5			<0.05
H_2O_2 concentration, mg/L c(H_2O_2)/c(DQO)	2 (0.016)	20 (0.16)	100 (0.08)	200 (1.6)	400 (3.2)	
%R (color)	69.5	74.2	76.2	88.5	86.3	<0.05
TiO_2 concentration, g/L	2	4	8	12		
%R (color)	62.7	77.2	88.5	87.7		<0.05
Dilution	1:4	1:3	1:2	1:1		
%R (color)	88.5	77.3	61.3	48.1		<0.05
UVC, μW/cm^2	1554	2801				
%R (color)	88.5	88.7				<0.05

The optimal conditions for color removal of the electrocoagulation pre-treated leachate through UVC photocatalytic processes with suspended TiO_2 are as follows: pH 5.6; c(H_2O_2)/c(COD) = 1.6; c(TiO_2) = 8 g/L; DIL 1:4; and UVC intensity = 2801 μW/cm^2. Table 6 presents the characterization of leachates treated by TiO_2–UVC photocatalysis with hydrogen peroxide (H_2O_2) at concentrations of 130 mg/L and 800 mg/L.

The combined electrocoagulation–photocatalysis treatment demonstrated high removal efficiencies for most pollutants. The application of hydrogen peroxide (H_2O_2) at different concentrations, 130 mg/L (H_2O_2/COD ratio of 0.27) and 800 mg/L (H_2O_2/COD ratio of 1.6) resulted in high removal efficiencies for COD (77.4–81.8%), ammonia (88.0–88.7%), and total phosphorus (94.3–94.4%). These results indicate that UVC/TiO_2 photocatalysis effectively removes refractory organic compounds and nitrogenous pollutants. On the other hand, increasing the H_2O_2 concentration did not significantly enhance removal efficiency, likely due to radical scavenging effects [22]. Regarding nitrogen removal, the process achieved an 88.0–88.7% reduction in ammonia and an 82.3–82.4% reduction in total nitrogen, values comparable to those reported by Del Moro et al. [26], where the integration of UV/H_2O_2 with biological treatment improved nitrogen removal.

Furthermore, heavy metals removal exceeded 80% in Zn, Fe, Pb, Mn, and Cu, and there was nearly complete removal of Cr^{6+} (95–100%). These results highlight the efficiency of combined electrocoagulation–photocatalysis in metal removal [33]. Specifically, Cr^{6+} (0.006 mg/L), Fe (0.07 mg/L), Cu (0.010 mg/L), Pb (0.134 mg/L), Mn (0.40 mg/L), and Zn (0.48 mg/L) levels meet regulatory limits, indicating that the treatment effectively controls these contaminants.

Table 6. Characterization of leachate treated by TiO_2/UVC photocatalysis compared to Ecuadorian regulations.

Parameter (%Removal)	Units	Leachate 130 mg H_2O_2/L (H_2O_2/COD Ratio of 0.27) (%Removal)	Leachate 800 mg H_2O_2/L (H_2O_2/COD Ratio of 1.6) (%Removal)	Ecuadorian Freshwater Body Regulations
pH		8.04	8.20	6–9
Color	PCU	114.7 (98.5%)	90.0 (98.8%)	-
COD	mg/L	310 (77.4%)	230 (81.8%)	200
BOD_5	mg/L	250 (33.9%)	250 (33.9%)	100
Total Solids (TS)	mg/L	20,321 (−58.3%)	19,501 (−51.9%)	1600
Total Nitrogen (TN)	mg/L	69.5 (82.3%)	69.0 (82.4%)	-
Ammonia (NH_3-N)	mg/L	24.1 (88.0%)	22.7 (88.7%)	30
Total Phosphorus (TP)	mg/L	5.1 (94.3%)	5.0 (94.4%)	10
Cr_{TOTAL}	mg/L	0.0235 (97.5%)	0.0519 (94.6%)	-
Cr^{6+}	mg/L	n/d (100%)	0.006 (95%)	0.5
Zn	mg/L	0.34 (86.9%)	0.48 (81.5%)	5
Fe	mg/L	0.21 (87.6%)	0.07 (95.9%)	10
Pb	mg/L	0.139 (78.0%)	0.134 (78.8%)	0.2
Mn	mg/L	0.40 (99.6%)	0.40 (99.6%)	2
Cu	mg/L	0.017 (98.3%)	0.010 (99.0%)	1

n/d = not detected.

3.4. Continuous Photocatalytic Treatment Using Immobilized TiO_2

Photocatalytic treatment using sand-immobilized TiO_2 demonstrated high efficiency in removing both chemical oxygen demand (COD) and color from electrocoagulation pre-treated leachate in a batch reactor. The treatment was conducted in a shallow Petri-type glass reactor (11 cm diameter and 1 cm height; see Figure 3), containing a uniform layer of sand coated with 1 g of TiO_2 per 100 g of sand. The leachate was irradiated with UVC light at an intensity of 2801 $\mu W/cm^2$ (wavelengths 180–254 nm, Toshiba 38 W lamp), with continuous agitation provided by a magnetic stirrer. The process was operated at an optimized pH of 5.6 and supplemented with 800 mg/L of H_2O_2 to enhance hydroxyl radical generation. After 2 h of UVC–TiO_2 treatment, COD was reduced from 520 mg/L to 98 mg/L, corresponding to an 81% removal efficiency. Additionally, color removal reached 93%, lowering the concentration from 4765 PCU to 333 PCU. These results are consistent with those reported by Wang et al. [22], who identified similar optimal conditions for the UV-TiO_2 process applied to aged landfill leachate, achieving 85% COD and 87.5% color removal through effective photocatalytic degradation.

In contrast, the continuous-flow photocatalytic treatment using sand-immobilized TiO_2 was applied to electrocoagulated and pre-filtered leachate (1 µm), following 12 h of aeration to reduce ammonium content. The system operated at an optimized pH of 5.6, with a TiO_2 loading of 1 g per 100 g of sand and was irradiated with UVC light at approximately 700 $\mu W/cm^2$ (180–254 nm), limited by the reactor configuration. As illustrated in Figure 4, the reactor contained approximately 4 L of TiO_2-coated sand (40% porosity), arranged in 12 internal zigzag channels (2 cm wide and 2 cm sand depth) to maximize contact between the leachate and the catalyst surface. A 1:10 diluted leachate stream was processed at a flow

rate of 5 mL/min using peristaltic pumps, providing a hydraulic retention time of about 4 h. Additionally, 80 mg/L of H_2O_2 was added to promote hydroxyl radical generation and enhance the degradation of recalcitrant organic contaminants under continuous UVC exposure. After 4 h of treatment, the system achieved a 49% reduction in COD. As shown in Figure 6, COD removal efficiencies in the continuous reactor ranged between 30% and 60%, depending on operational conditions.

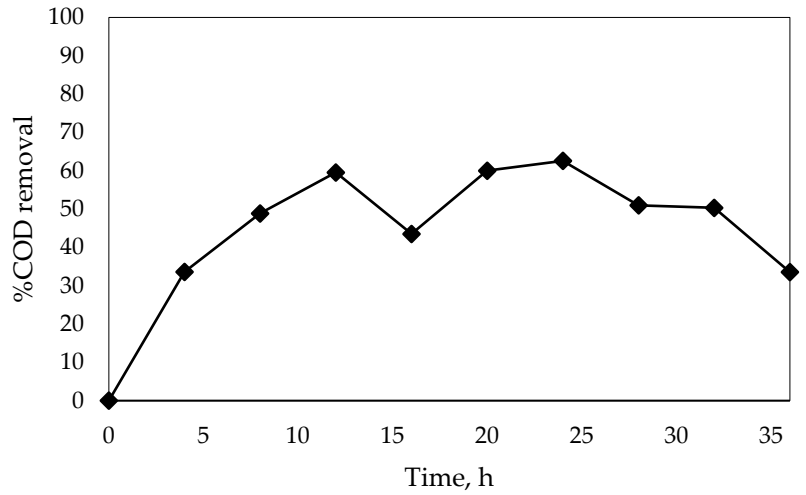


Figure 6. COD removal efficiency over time in a continuous reactor.

The reduced performance observed in the continuous-flow photocatalytic treatment—compared to batch systems—can be attributed to several factors related to reactor design and operational conditions [39]. A key issue is the initial adsorption of organic pollutants and their oxidation byproducts in the inlet sections of the reactor, which reduces the availability of active catalytic surfaces and thereby limits photocatalytic efficiency [40]. Additionally, the lower radiation intensity (~700 μW/cm^2) in the continuous reactor may diminish TiO_2 activation and reduce degradation efficiency [41]. As noted by Colmenares and Xu [39], insufficient light intensity significantly limits the formation of reactive oxygen species and hinders photocatalytic performance, particularly in scaled-up or fixed-bed systems. Moreover, the absence of intense agitation—unlike in batch configurations—further decreases mass transfer rates, as demonstrated by Hänel et al. [40], who reported substantially lower phenol degradation efficiencies in fixed-bed reactors with immobilized TiO_2 compared to suspended systems, mainly due to restricted surface accessibility and limited mass transfer under static conditions.

However, color removal was highly effective, achieving a 98% reduction. Figure 7 illustrates the behavior of color removal efficiency in the treatment of leachates. The results indicate a highly efficient process in terms of color removal.

During the initial hours, color removal reaches over 99%, suggesting a high initial efficiency of the system. This behavior can be attributed to the initial adsorption of chromophoric compounds onto the catalytic material. Additionally, UVC irradiation promotes the generation of reactive species, such as hydroxyl radicals, which effectively attack the chromophoric bonds responsible for coloration—an effect consistent with the findings of Chairungsri et al. [42], who reported up to 93.7% color removal in batch systems and sustained efficiencies of 67.8–80.2% in continuous reactors using TiO_2-coated glass beads for textile dye degradation.

Compared to COD removal, color elimination appears to be notably more efficient and stable. This difference may be explained by variations in their respective removal mechanisms. While color removal may be dominated by adsorption processes and di-

rect photocatalytic attacks on chromophoric structures, COD elimination is more strongly affected by operational limitations—such as TiO_2 fixation on sand—and especially by the more complex reaction mechanisms required for complete mineralization. This behavior was also reported by Panizza and Cerisola [43], who observed nearly complete decolorization of alizarin red and over 90% COD removal using an Electro-Fenton process (AOP), highlighting that chromophore degradation tends to occur more rapidly than full mineralization of organic matter, even under highly oxidative conditions.

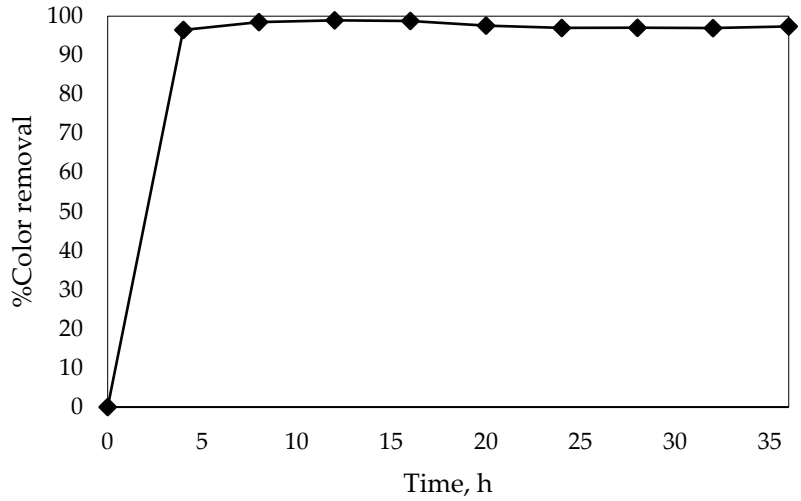


Figure 7. Color removal efficiency over time in a continuous reactor.

Furthermore, these findings are consistent with previous studies on UVC–TiO_2 photocatalysis, which indicate that batch reactors may outperform continuous-flow systems under specific configurations—particularly when catalyst immobilization, poor mixing, or short residence times limit the efficiency of pollutant–catalyst interaction [44,45]. Nevertheless, the literature highlights the superior scalability of continuous reactors for large-scale applications, provided that operational challenges such as catalyst fouling and inefficient hydrodynamics are adequately addressed. In this context, Jadaa et al. [46] demonstrated that mass transfer limitations and surface site saturation are key constraints in heterogeneous immobilized TiO_2 systems, significantly hindering degradation efficiency in the absence of sufficient mixing and surface renewal. Additionally, recent studies on UV-LED/TiO_2 photocatalysis have reported promising results in the degradation of organic micropollutants, offering energy-efficient alternatives to conventional UV systems [47]. Taken together, these insights suggest that while batch photocatalysis with immobilized TiO_2 is highly effective for organic degradation, further advances in reactor design—particularly strategies that enhance surface renewal and mitigate mass transfer limitations—could substantially improve the performance and scalability of continuous systems for real-world leachate treatment scenarios [48].

3.5. Surface Characterization of TiO_2-Coated Sand by Scanning Electron Microscopy and EDS Mapping

Scanning electron microscopy (SEM) images combined with energy-dispersive X-ray spectroscopy (EDS) confirmed the successful but heterogeneous deposition of TiO_2 onto the porous sand substrate.

Low-magnification micrographs (Figure 8a,b, 140–730×) reveal a rough, granular morphology characterized by numerous interconnected cavities. Specifically, the 730× image shows pore diameters ranging from 24.5 μm to 88.7 μm, forming a complex porous network conducive to catalyst retention and fluid transport—favorable conditions for photocatalytic

interaction. High-magnification SEM images (Figure 8c,d, 5800× and 6700×) reveal angular crystalline agglomerates adhered to the inner pore walls. These light-toned structures are consistent with TiO_2 clusters, often embedded within surface irregularities, suggesting strong mechanical anchoring without significant obstruction of the pore structure.

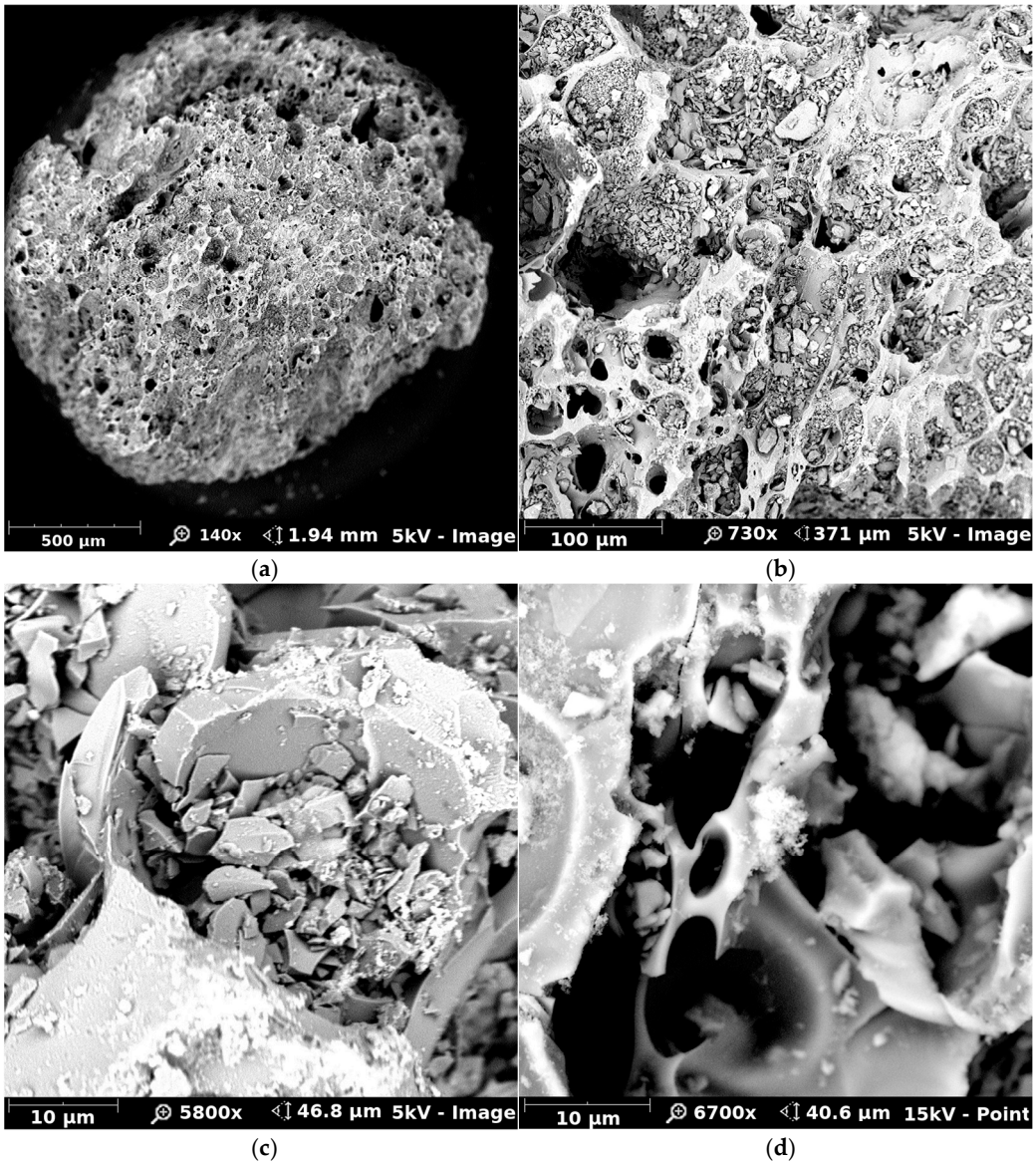


Figure 8. SEM micrographs of TiO_2-coated sand at increasing magnifications. (**a**) 140×: granular surface with roughness favorable for catalyst anchoring; (**b**) 730×: pore diameters from 24.5 to 88.7 µm; (**c**) 5800×: TiO_2 agglomerates attached to inner pore walls; and (**d**) 6700×: dense TiO_2 clusters embedded in surface irregularities.

EDS elemental analysis (Figure 9a) confirms the presence of titanium across the surface, with an average concentration of 1.7 wt%. Signals from O, Si, Al, Na, and K reflect the aluminosilicate nature of the sand. The results reveal a discontinuous and scattered Ti distribution, indicating a non-uniform coating. Point analysis (Figure 9b) identified localized areas with high titanium content (up to 14.6 wt%), suggesting TiO_2 accumulation in topographically favorable regions such as pores and depressions. In contrast, other points showed negligible or undetectable Ti levels, further confirming the heterogeneity of the coating.

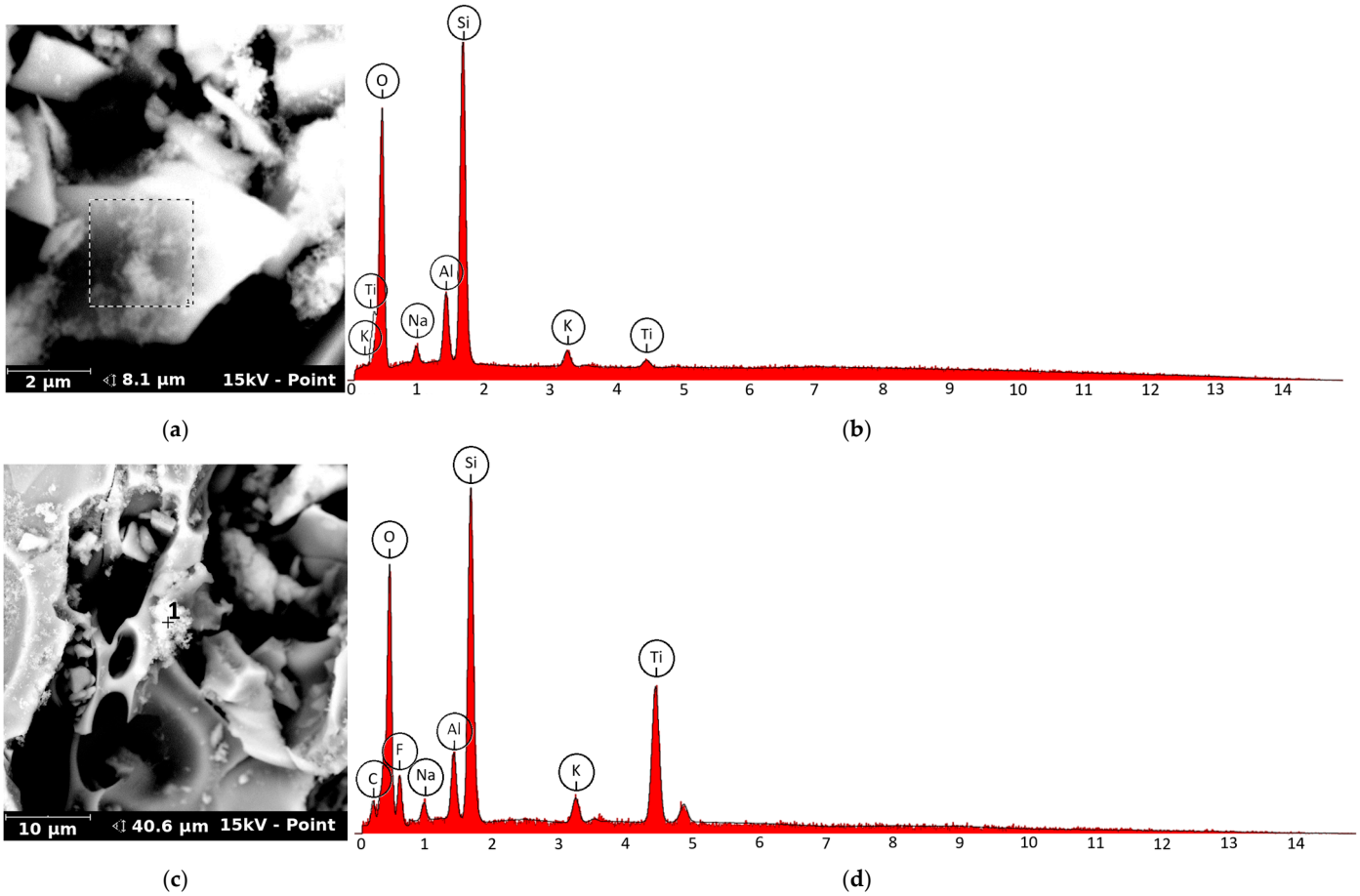


Figure 9. EDS elemental analysis of TiO_2-coated sand. (**a**) SEM micrograph showing an uncoated region of the support. (**b**) EDS spectrum corresponding to (**a**), with Si, O, Al, K, and Na signals that indicate the aluminosilicate matrix and confirm the absence of Ti. (**c**) SEM image of an internal pore wall with visible TiO_2 agglomeration; the marked point (1) indicates the site of elemental analysis. (**d**) EDS spectrum corresponding to (**c**), displaying strong Ti signal along with Si and O, confirming localized TiO_2 deposition.

Overall, the SEM–EDS results confirm the morphological suitability of the porous sand support for TiO_2 immobilization, as its rough and interconnected surface facilitates strong mechanical anchoring of the photocatalyst. This observation is consistent with findings by Hanaor and Sorrell [49], who reported that TiO_2 coatings on quartz sand exhibit excellent mechanical stability, a uniform nanocrystalline morphology (30–50 nm), and a mixed anatase–rutile phase that promotes effective charge carrier separation and enhances overall photocatalytic activity. These results underscore the importance of both substrate selection and coating technique optimization to ensure the long-term performance and stability of immobilized TiO_2 systems in practical applications; however, additional characterization techniques such as X-ray diffraction (XRD) and Fourier-transform infrared spectroscopy (FTIR) may provide further insights into phase transitions or structural changes induced by the calcination process [50].

4. Conclusions

The physicochemical and heavy metal characterization of the raw biocell leachate generated under laboratory-scale conditions revealed pollutant concentrations that significantly exceed Ecuadorian discharge regulations, indicating a high potential environmental risk if such effluents were released untreated into natural systems. Elevated COD (1373 mg/L) and BOD_5 (378 mg/L) levels indicate substantial organic pollution with low biodegrad-

ability (BOD_5/COD ratio of 0.28), while excessive total solids (12,835 mg/L), phosphorus (90 mg/L), and nitrogen species—particularly ammoniacal nitrogen (201 mg/L) and total nitrogen (393 mg/L)—raise significant concerns regarding aquatic toxicity and eutrophication. The leachate also displayed critical exceedances in nickel (+253%), lead (+216%), manganese (+134%), and cadmium (+115%), likely attributed to the co-disposal of metal-rich sludge from the Ambato WWTP, distinguishing this matrix from typical landfill leachates.

Electrocoagulation treatment of the leachate achieved efficient removal of key pollutants, including 62.6% COD, 44.4% BOD_5, and 89.8% total phosphorus, while maintaining a favorable energy consumption profile at 500 mA. However, although color and total nitrogen removal were significant (86.2% and 38.9%, respectively), ammoniacal nitrogen removal (17.9%) remained insufficient to meet discharge limits. Energy optimization experiments confirmed that excessively high current intensities diminished process efficiency due to increased side reactions and electrode passivation. Nonetheless, metal removal was highly effective, with lead, cadmium, and copper reduced below regulatory thresholds, and Cr^{6+} reaching compliant levels despite moderate removal efficiency. These results support the robustness of electrocoagulation for metal and phosphorus removal, though they highlight the need for supplementary processes to address nitrogenous pollutants.

Coupling electrocoagulation with UVC/TiO_2 photocatalysis resulted in superior treatment performance, with COD reductions of 77.4–81.8%, ammonia removal of 88.0–88.7%, and phosphorus elimination above 94%. Optimal photocatalytic conditions—pH 5.6, TiO_2 concentration of 8 g/L, 1:4 dilution, H_2O_2/COD ratio of 1.6, and UVC intensity of 2801 $\mu W/cm^2$—enabled enhanced degradation of refractory organics and nutrient species. Overdosing H_2O_2 was found counterproductive due to radical scavenging effects. Heavy metals including Zn, Fe, Pb, Mn, and Cu showed >80% removal, and Cr^{6+} was nearly completely eliminated, ensuring full compliance with discharge regulations. These findings confirm that integrating electrocoagulation with UVC/TiO_2 photocatalysis is a technically and environmentally sound strategy for advanced leachate remediation.

SEM–EDS analysis of the TiO_2-coated sand demonstrated the morphological suitability of the substrate, with its rough and porous surface promoting strong catalyst adhesion within internal cavities. However, titanium was found to be heterogeneously distributed, with localized enrichment (up to 14.6 wt%) and regions lacking detectable Ti, which could compromise photocatalytic efficiency. These results highlight the need to refine the coating methodology to ensure uniform TiO_2 dispersion—particularly critical for dynamic reactor configurations.

In conclusion, the integrated electrocoagulation–photocatalysis strategy proved effective for complex biocell leachate treatment, addressing both organic and inorganic contaminants. Yet, achieving stable and scalable application will depend on further optimizing catalyst support materials, reactor configuration, and operational parameters to ensure consistent, cost-effective, and regulatory-compliant performance in real-world contexts.

Author Contributions: Conceptualization, R.P.; methodology, R.P., F.R.L.C., L.P., and C.M.M.R.; validation, R.P. and N.E.F.T.; formal analysis, N.E.F.T. and R.P.; investigation, N.E.F.T., R.P., L.P, and C.M.M.R.; resources, R.P.; data curation, N.E.F.T.; writing—original draft preparation, N.E.F.T., R.P., and L.P.; writing—review and editing, N.E.F.T. and R.P.; visualization, R.P. and F.R.L.C.; supervision, R.P.; project administration, R.P. and C.M.M.R.; and funding acquisition, R.P. and N.E.F.T. All authors have read and agreed to the published version of the manuscript.

Funding: This research was funded by the Ecuadorian Corporation for Research and Academia Development (CEDIA) through the IDi Fund Universities, IDi XVIII 2023, and was carried out as part of the Project I+D+I-XVIII-2023-50: "Development of a Toxicological Testing Platform in Zebrafish (Danio rerio) for the Discovery of New Environmental Contaminants and the Evaluation of Water

Quality to Assess the Effectiveness of Decontamination Treatments". We also extend our gratitude to the Research and Development Directorate (DIDE), the Faculty of Food Science and Biotechnology Engineering, Universidad Técnica de Ambato, Ecuador (FCIAB), and the Universidad Técnica de Ambato (UTA), Ambato, Ecuador for their support as part of the Project "Descontaminación de aguas residuales industriales en la Provincia de Tungurahua con Métodos electroquímicos combinados con fitorremediación"; PFCIAL 40.

Data Availability Statement: No data were generated or analyzed during the current study.

Acknowledgments: The authors thank Dirección de Investigación y Desarrollo (DIDE) and the Technical University of Ambato–Ecuador for support through the project's financial approval by resolution "Descontaminación de aguas residuales industriales en la Provincia de Tungurahua con métodos electroquímicos combinados con fitorremediación" (Resolution No. UTA-CONIN-2024-0194-R). The authors gratefully acknowledge the Ambato Municipal Water and Sanitation Company (EP-EMAPA-A) and the Wastewater Treatment Plant (WWTP) in Ambato, Ecuador, for their valuable support throughout the development of this project and for providing the biosolid samples used in this study. The authors also thank the Gestión de Recursos Naturales e Infraestructura Sustentable (GeReNIS) research group and the G+ Bio-Food and Engineering research group, both affiliated with the Universidad Técnica de Ambato, Ecuador, for their technical guidance and constructive suggestions. Additional support from the project "Canje de Deuda Ecuador–España: Fortalecimiento de la Unidad Operativa de Investigación (FITA–UOITA)", Faculty of Food Science and Biotechnology Engineering, Universidad Técnica de Ambato, is gratefully acknowledged. Finally, the authors are thankful to NanoInstrumentos Ecuador for their technical assistance and for providing access to the Phenom ProX G6 desktop scanning electron microscope.

Conflicts of Interest: The authors declare no conflicts of interest.

Abbreviations

The following abbreviations are used in this manuscript:

WWTP	Wastewater treatment plant
EC	Electrocoagulation
UVC	Ultraviolet C
COD	Chemical oxygen demand
BOD	Biochemical oxygen demand
POPs	Persistent organic pollutants
PC	Photocatalysis
SM	Standard Methods
APHA	American Public Health Association
TULSMA	Unified Text of Secondary Environmental Legislation (Ecuador)
SEM	Scanning electron microscopy
EDS	Energy-dispersive X-ray spectroscopy
BSD	Backscattered Electron Detector
TN	Total nitrogen
ANOVA	Analysis of Variance
%R	Percent Removal

References

1. Das, R.; Raj, D. Sources, distribution, and impacts of emerging contaminants—A critical review on contamination of landfill leachate. *J. Hazard. Mater. Adv.* **2025**, *17*, 100602. [CrossRef]
2. Mor, S.; Ravindra, K.; Dahiya, R.P.; Chandra, A. Leachate characterization and assessment of groundwater pollution near municipal solid waste landfill site. *Environ. Monit. Assess.* **2006**, *118*, 435–456. [CrossRef]
3. Ministerio del Ambiente y Agua del Ecuador. Manual de Aprovechamiento de Residuos Orgánicos Municipales. Quito; 2020. Available online: https://www.ambiente.gob.ec/wp-content/uploads/downloads/2020/07/MANUAL-DE-APROVECHAMIENTO-DE-RESIDUOS-ORGANICOS-MUNICIPAL.pdf (accessed on 3 February 2025).

4. EPA. Bioreactor Landfills. 2023. Available online: https://www.epa.gov/landfills/bioreactor-landfills (accessed on 3 February 2025).
5. Hettiaratchi, J.P.A. Landfill Bioreactors. In *Encyclopedia of Sustainability Science and Technology*; Springer: New York, NY, USA, 2012; pp. 5720–5732.
6. Baun, A.; Ledin, A.; Reitzel, L.A.; Bjerg, P.L.; Christensen, T.H. Xenobiotic organic compounds in leachates from ten Danish MSW landfills—Chemical analysis and toxicity tests. *Water Res.* **2004**, *38*, 3845–3858. [CrossRef] [PubMed]
7. Kjeldsen, P.; Barlaz, M.A.; Rooker, A.P.; Baun, A.; Ledin, A.; Christensen, T.H. Present and long-term composition of MSW landfill leachate: A review. *Crit. Rev. Environ. Sci. Technol.* **2002**, *32*, 297–336. [CrossRef]
8. Jamrah, A.; AL-Zghoul, T.M.; Al-Qodah, Z. An Extensive Analysis of Combined Processes for Landfill Leachate Treatment. *Water* **2024**, *16*, 1640. [CrossRef]
9. Mollah, Y.M.; Schennach, R.; Parga, J.R.; Cocke, D.L. Electrocoagulation (EC)-science and applications. *J. Hazard. Mater.* **2001**, *84*, 29–41. [CrossRef]
10. Zailani, L.W.M.; Zin, N.S.M. Application of Electrocoagulation in Various Wastewater and Leachate Treatment-A Review. In *IOP Conference Series: Earth and Environmental Science*; Institute of Physics Publishing: Bristol, UK, 2018.
11. Chen, D.; Cheng, Y.; Zhou, N.; Chen, P.; Wang, Y.; Li, K.; Huo, S.; Cheng, P.; Peng, P.; Zhang, R.; et al. Photocatalytic degradation of organic pollutants using TiO_2-based photocatalysts: A review. *J. Clean. Prod.* **2020**, *268*, 121725. [CrossRef]
12. Ibhadon, A.O.; Fitzpatrick, P. Heterogeneous photocatalysis: Recent advances and applications. *Catalysts* **2013**, *3*, 189–218. [CrossRef]
13. Li, X.; Wei, H.; Song, T.; Lu, H.; Wang, X. A review of the photocatalytic degradation of organic pollutants in water by modified TiO_2. *Water Sci. Technol.* **2023**, *88*, 1495–1507. [CrossRef]
14. Fujishima, A.; Zhang, X. Titanium dioxide photocatalysis: Present situation and future approaches. *Comptes Rendus Chim.* **2006**, *9*, 750–760. [CrossRef]
15. Yarbay, R.Z.; Şimşek, V.; Bogdan, L.; Tomašić, V. Photocatalytic Degradation of Neonicotinoids—A Comparative Study of the Efficacy of Hybrid Photocatalysts. *Processes* **2024**, *12*, 489. [CrossRef]
16. Anucha, C.B.; Bacaksiz, E.; Stathopoulos, V.N.; Pandis, P.K.; Argirusis, C.; Andreouli, C.D.; Tatoudi, Z.; Altin, I. Molybdenum Modified Sol–Gel Synthesized TiO_2 for the Photocatalytic Degradation of Carbamazepine under UV Irradiation. *Processes* **2022**, *10*, 1113. [CrossRef]
17. Ates, H.; Dizge, N.; Yatmaz, H.C. Combined process of electrocoagulation and photocatalytic degradation for the treatment of olive washing wastewater. *Water Sci. Technol.* **2017**, *75*, 141–154. [CrossRef] [PubMed]
18. APHA. *Standard Methods for the Examination of Water and Wastewater*, 23rd ed.; American Public Health Association: Washington, DC, USA, 2017.
19. Ministerio del Ambiente del Ecuador. Texto Unificado de Legislación Secundaria del Ministerio del Ambiente: Libro VI, Anexo 1—Norma de Calidad Ambiental y de Descarga de Efluentes al Recurso Agua. Registro Oficial Suplemento 387. 2015. Available online: https://www.gob.ec/sites/default/files/regulations/2018-09/Documento_Registro-Oficial-No-387-04-noviembre-2015_0.pdf (accessed on 9 February 2025).
20. Hettiaratchi, J.P.A.; Jayasinghe, P.A.; Bartholameuz, E.M.; Kumar, S. Waste degradation and gas production with enzymatic enhancement in anaerobic and aerobic landfill bioreactors. *Bioresour. Technol.* **2014**, *159*, 433–436. [CrossRef]
21. Luo, H.; Zeng, Y.; Cheng, Y.; He, D.; Pan, X. Recent advances in municipal landfill leachate: A review focusing on its characteristics, treatment, and toxicity assessment. *Sci. Total Environ.* **2020**, *703*, 135468. [CrossRef] [PubMed]
22. Wang, J.; Qiao, Z. A comprehensive review of landfill leachate treatment technologies. *Front. Environ. Sci.* **2024**, *12*, 1439128. [CrossRef]
23. Lacerda, J.A.; Macedo, A.M.; Teixeira, R.I.; Simões, G.; Ribeiro, E.S.; Forero, J.S.; Corrêa, R.J. TiO_2 Decorated Sand Grains for Photodegradation of Pollutants: Methylene Blue and Ciprofloxacin Study. *J. Braz. Chem. Soc.* **2020**, *31*, 201–210. [CrossRef]
24. Sulaiman, F.; Alwared, A. Ability of Response Surface Methodology to Optimize Photocatalytic Degradation of Amoxicillin from Aqueous Solutions Using Immobilized TiO_2/Sand. *J. Ecol. Eng.* **2022**, *23*, 293–304. [CrossRef]
25. Sancha, M. Caracterización y Tratamiento de Lixiviados Generados en Vertederos de Residuos Urbanos. Available online: http://www.unioviedo.es/MBTA (accessed on 9 February 2025).
26. Del Moro, G.; Mancini, A.; Mascolo, G.; Di Iaconi, C. Comparison of UV/H_2O_2 based AOP as an end treatment or integrated with biological degradation for treating landfill leachates. *Chem. Eng. J.* **2013**, *218*, 133–137. [CrossRef]
27. Manahan, S.E. *Environmental Chemistry*, 11th ed.; CRC Press: Boca Raton, FL, USA, 2022.
28. Ali, Z.; Yousafzai, A.M.; Sher, N.; Muhammad, I.; Nayab, G.E.; Aqeel, S.A.M.; Shah, S.T.; Aschner, M.; Khan, I.; Khan, H. Toxicity and bioaccumulation of manganese and chromium in different organs of common carp (Cyprinus carpio) fish. *Toxicol. Rep.* **2021**, *8*, 343–348. [CrossRef]
29. Ingelsson, M.; Yasri, N.; Roberts, E.P.L. Electrode passivation, faradaic efficiency, and performance enhancement strategies in electrocoagulation—A review. *Water Res.* **2020**, *187*, 116433. [CrossRef] [PubMed]

30. Jallouli, S.; Wali, A.; Buonerba, A.; Zarra, T.; Belgiorno, V.; Naddeo, V.; Ksibi, M. Efficient and sustainable treatment of tannery wastewater by a sequential electrocoagulation-UV photolytic process. *J. Water Process Eng.* **2020**, *38*, 101642. [CrossRef]
31. Mollah, M.Y.A.; Morkovsky, P.; Gomes, J.A.G.; Kesmez, M.; Parga, J.; Cocke, D.L. Fundamentals, present and future perspectives of electrocoagulation. *J. Hazard. Mater.* **2004**, *114*, 199–210. [CrossRef] [PubMed]
32. Rookesh, T.; Samaei, M.R.; Yousefinejad, S.; Hashemi, H.; Derakhshan, Z.; Abbasi, F.; Jalili, M.; Giannakis, S.; Bilal, M. Investigating the Electrocoagulation Treatment of Landfill Leachate by Iron/Graphite Electrodes: Process Parameters and Efficacy Assessment. *Water* **2022**, *14*, 205. [CrossRef]
33. Khan, S.U.; Khalid, M.; Hashim, K.; Jamadi, M.H.; Mousazadeh, M.; Basheer, F.; Farooqi, I.H. Efficacy of Electrocoagulation Treatment for the Abatement of Heavy Metals: An Overview of Critical Processing Factors, Kinetic Models and Cost Analysis. *Sustainability* **2023**, *15*, 1708. [CrossRef]
34. Valencia, S.H.; Marín, J.M.; Restrepo, G.M. Efecto del pH en la Degradación Fotocatalítica de Materia Orgánica Natural. *Inf. Tecnol.* **2011**, *22*, 57–66. [CrossRef]
35. Harun, N.; Sheng, C.K.; Sabri, M.G.M.; Dagang, A.N.; Salleh, H. Impact of TiO_2 and H_2O_2 on Photocatalytic Degradation of Rhodamine B under Ultraviolet C (UV-C) Radiation for Efficient Polluted Wastewater Treatment. *J. Optoelectron. Biomed. Mater.* **2020**, *12*, 9–15. [CrossRef]
36. Kim, S.Y.; Lee, T.G.; Hwangbo, S.A.; Jeong, J.R. Effect of the TiO_2 Colloidal Size Distribution on the Degradation of Methylene Blue. *Nanomaterials* **2023**, *13*, 302. [CrossRef]
37. Poulopoulos, S.G.; Yerkinova, A.; Ulykbanova, G.; Inglezakis, V.J. Photocatalytic treatment of organic pollutants in a synthetic wastewater using UV light and combinations of TiO_2, H_2O_2 and Fe(III). *PLoS ONE* **2019**, *14*, e0216745. [CrossRef]
38. Ahmed, S.N.; Haider, W. Heterogeneous photocatalysis and its potential applications in water and wastewater treatment: A review. *Nanotechnology* **2018**, *29*, 342001. [CrossRef]
39. Colmenares, J.C.; Xu, Y.J. (Eds.) *Heterogeneous Photocatalysis*; Springer: Berlin/Heidelberg, Germany, 2016.
40. Hänel, A.; Zaleska, A.; Hupka, J. Photocatalytic activity of TiO_2 immobilized on glass beads. *Physicochem. Probl. Miner. Process.* **2010**, *45*, 49–56. Available online: https://www.researchgate.net/publication/279628443 (accessed on 9 February 2025).
41. Umar, M.; Abdul, H. Photocatalytic Degradation of Organic Pollutants in Water. In *Organic Pollutants—Monitoring, Risk and Treatment*; IntechOpen Limited: London, UK, 2013.
42. Chairungsri, W.; Pholchan, P.; Sumitsawan, S.; Chimupala, Y.; Kijjanapanich, P. Photocatalytic Degradation of Textile Dyeing Wastewater Using Titanium Dioxide on a Fixed Substrate: Optimization of Process Parameters and Continuous Reactor Tests. *Sustainability* **2023**, *15*, 12418. [CrossRef]
43. Panizza, M.; Cerisola, G. Electro-Fenton degradation of synthetic dyes. *Water Res.* **2009**, *43*, 339–344. [CrossRef]
44. Rahimi, S.; Poormohammadi, A.; Salmani, B.; Ahmadian, M.; Rezaei, M. Comparing the photocatalytic process efficiency using batch and tubular reactors in removal of methylene blue dye and COD from simulated textile wastewater. *J. Water Reuse Desalination* **2016**, *6*, 574–582. [CrossRef]
45. Colombo, E.; Ashokkumar, M. Comparison of the photocatalytic efficiencies of continuous stirred tank reactor (CSTR) and batch systems using a dispersed micron sized photocatalyst. *RSC Adv.* **2017**, *7*, 48222–48229. [CrossRef]
46. Jadaa, W.; Prakash, A.; Ray, A.K. Photocatalytic Degradation of Diazo Dye over Suspended and Immobilized TiO_2 Catalyst in Swirl Flow Reactor: Kinetic Modeling. *Processes* **2021**, *9*, 1741. [CrossRef]
47. Bertagna Silva, D.; Buttiglieri, G.; Babić, S. State-of-the-art and current challenges for TiO_2/UV-LED photocatalytic degradation of emerging organic micropollutants. *Environ. Sci. Pollut. Res.* **2021**, *28*, 103–120. [CrossRef]
48. Enesca, A. The Influence of Photocatalytic Reactors Design and Operating Parameters on the Wastewater Organic Pollutants Removal—A Mini-Review. *Catalysts* **2021**, *11*, 556. [CrossRef]
49. Hanaor, D.A.H.; Sorrell, C.C. Sand Supported Mixed-Phase TiO_2 Photocatalysts for Water Decontamination Applications Decontamination Applications. *Adv. Eng. Mater.* **2014**, *16*, 248–254. [CrossRef]
50. Kim, M.G.; Kang, J.M.; Lee, J.E.; Kim, K.S.; Kim, K.H.; Cho, M.; Lee, S.G. Effects of Calcination Temperature on the Phase Composition, Photocatalytic Degradation, and Virucidal Activities of TiO_2 Nanoparticles. *ACS Omega* **2021**, *6*, 10668–10678. [CrossRef]

Disclaimer/Publisher's Note: The statements, opinions and data contained in all publications are solely those of the individual author(s) and contributor(s) and not of MDPI and/or the editor(s). MDPI and/or the editor(s) disclaim responsibility for any injury to people or property resulting from any ideas, methods, instructions or products referred to in the content.